

## Immune phase transition under steroid treatment

Sonali Priyadarshini Nayak <sup>1</sup> and Susmita Roy <sup>2,\*</sup>

<sup>1</sup>*College of Integrated Studies, University of Hyderabad, Hyderabad, Telangana 500046, India*

<sup>2</sup>*Department of Chemical Sciences, Indian Institute of Science Education and Research Kolkata, Campus Road, Mohanpur, West Bengal 741246, India*



(Received 3 December 2020; revised 8 April 2021; accepted 11 May 2021; published 3 June 2021)

The steroid hormone glucocorticoid (GC) is a well-known immunosuppressant that controls T-cell-mediated adaptive immune response. In this work, we have developed a minimal kinetic network model of T-cell regulation connecting relevant experimental and clinical studies to quantitatively understand the long-term effects of GC on pro-inflammatory T-cell ( $T_{\text{pro}}$ ) and anti-inflammatory T-cell ( $T_{\text{anti}}$ ) dynamics. Due to the antagonistic relation between these two types of T cells, their long-term steady-state population ratio helps us to characterize three classified immune regulations: (i) weak ( $[T_{\text{pro}}] > [T_{\text{anti}}]$ ), (ii) strong ( $[T_{\text{pro}}] < [T_{\text{anti}}]$ ), and (iii) moderate ( $[T_{\text{pro}}] \sim [T_{\text{anti}}]$ ), holding the characteristic bistability. In addition to the differences in their long-term steady-state outcome, each immune regulation shows distinct dynamical phases. In the presteady state, a characteristic intermediate stationary phase is observed to develop only in the moderate regulation regime. In the medicinal field, the resting time in this stationary phase is distinguished as a clinical latent period. GC dose-dependent steady-state analysis shows an optimal level of GC to drive a phase transition from the weak or autoimmune prone to the moderate regulation regime. Subsequently, the presteady state clinical latent period tends to diverge near that optimal GC level where  $[T_{\text{pro}}] : [T_{\text{anti}}]$  is highly balanced. The GC-optimized elongated stationary phase explains the rationale behind the requirement of long-term immune diagnostics, especially when long-term GC-based chemotherapeutics and other immunosuppressive drugs are administrated. Moreover, our study reveals GC sensitivity of clinical latent period, which might serve as an early warning signal in diagnosing different immune phases and determining immune phase-wise steroid treatment.

DOI: [10.1103/PhysRevE.103.062401](https://doi.org/10.1103/PhysRevE.103.062401)

### I. INTRODUCTION

The dynamics of biological regulatory networks, their adaptation under different environmental stresses, and how they are misguided and diseased are all timely and relevant global questions [1–4]. For instance, in the current pandemic situation, our utmost focus lies on the human immune network, which undertakes a cascade of cellular interaction and biomolecular reactions to protect us against a universe of pathogenic microbes. The human immune system is a highly complex network where the immune cells are in continuous interactions and clashes with foreign invaders/pathogens to maintain a healthy state. One of the key targets of this immune system is to distinguish between self-cells and non-self-cells. In consideration of its way of operation, the immune response has two interconnected arms in the form of two subsystems, i.e., innate immunity and adaptive immunity. While the innate immune system is a nonspecific type of defense mechanism which is present in our body from the time of birth, adaptive immunity is a subsystem of the immune system which comprises specialized, systemic cells but a slow pace response process. Among different lymphocyte populations of the adaptive immune system, although CD4+ T cells play a significant role in the immune responses throughout the defense mechanism against the pathogen, on the contrary,

some pro-inflammatory CD4+ T cells often fail to distinguish between self- and non-self-cells, causing some autoimmune diseases and allergies. Among these CD4+ T cells, some act as pro-inflammatory cells, others as anti-inflammatory cells. The regulatory or anti-inflammatory T cells exert a downregulation mechanism on the population of effector or pro-inflammatory T cells to prevent auto-immunity [5–11].

The human body has a myriad of feedback loops and mechanisms to balance the dynamic equilibrium of the cell populations for the proper functionality of a healthy body. Along with the regulatory anti-inflammatory T cell, secosteroid hormonelike vitamin D and steroid hormonelike glucocorticoid (GC) [12–19] also evolve to supplement its immunomodulatory action. Vitamin D and GC both downregulate the pro-inflammatory T-cell population and upregulate the anti-inflammatory T-cell population [1,2,4,12–14,20–22]. In our early study, we have developed a coarse-grained but general kinetic model in an attempt to capture the immunomodulatory role of vitamin D to control the population ratio between pro-inflammatory and anti-inflammatory T-cell populations. We revealed a nonlinear effect of vitamin D on T-cell regulation, which is an indirect result of antigen presentation and subsequent production of pro-inflammatory effector T cells [4]. In subsequent work, borrowing concepts from equilibrium statistical mechanics, we introduced a description of the immune response function in terms of fluctuations in different subsets of T cells [3]. We found a divergencelike growth near the coexistence line of distinct

\*susmita.roy@iiserkol.ac.in

immune phases, which is a characteristic of dynamic phase transition. A phase transition phenomenon, in general, is coupled to an external perturbation. In our T-cell regulation model, we are focused on deriving the GC dose dependence of T-cell dynamics. Along with that, we also intend to draw a phase diagram delineating different immune phases over a sensitive order-parameter domain.

To envision a multidimensional phase diagram distinguishing different immune phases in the field of immunology is a relatively new concept compared to its wide range of applicability in physical chemistry, engineering, mineralogy, and materials science [23–26]. On the other hand, the framework of mathematical models dealing with cellular dynamics that drive the crossover from one phase to the other has long been one of the major topics in cell biology. In such studies, microbial cell growth dynamics are monitored under different environmental conditions. In the case of bacterial cell growth, the environmental drivers are oxygen,  $pH$ , temperature, or availability of nutrients, to name a few [27]. In a laboratory, under optimal conditions, a canonical microbial growth curve follows essentially four different phases: (i) lag phase, (ii) log phase, (iii) stationary phase, and (iv) death phase. The exponentially growing log phase has led to the development of several growth laws, while an emerging stationary phase is observed to halt the growth under critical environmental stress. Once cells enter the stationary phase, a certain time span is generally required to recover growth after the condition tends to renormalize [28–30].

In recent times, the dynamical pattern of  $CD4+$  T-cell counts of HIV-infected individuals has been monitored to follow the disease progression. For clinicians,  $CD4+$  T-cell count and viral levels in the plasma are the key markers to navigate the disease progression. Also, in such cases, after an acute infection period (2–10 weeks),  $CD4+$  T cells enter a stationary phase clinically termed as a “clinical latent phase.” This is an apparent near-normal asymptomatic phase, where viral load drops dramatically. However, in this phase, HIV is continuously infecting new cells and actively replicating. After a long asymptomatic period (more than 15 years as evidenced), the virus enters into a resurrection phase and eventually gets out of control to destroy the remaining cells [31,32]. A very recent kinetic model has attempted to characterize the role of GC on the immune system and antitumor immune response over a 30-day period under a constrained GC supply [33]. However, several early clinical reports suggest that most immunosuppressive and chemotherapeutic GC-based drugs at their high dose have a long-term (in terms of years) effect rather, and the adverse effect(s) of these drugs may arise even long after the treatment has stopped [34–36]. From the above cases, it is evident that long-term immune dynamics under GC administration need to be studied.

GC drugs have been used in the field of medicine for more than 65 years. Though there are several classes of cost-effective synthetic GCs, dexamethasone (dex) is the most widely used because of its higher binding affinity to GC receptors (GRs) than natural cortisol; additionally, it has minimal mineralocorticoid activity. However, it is much more potent and has a longer duration of action as compared to other synthetic GCs like prednisolone and prednisone [37–40]. GC exerts their primary anti-inflammatory

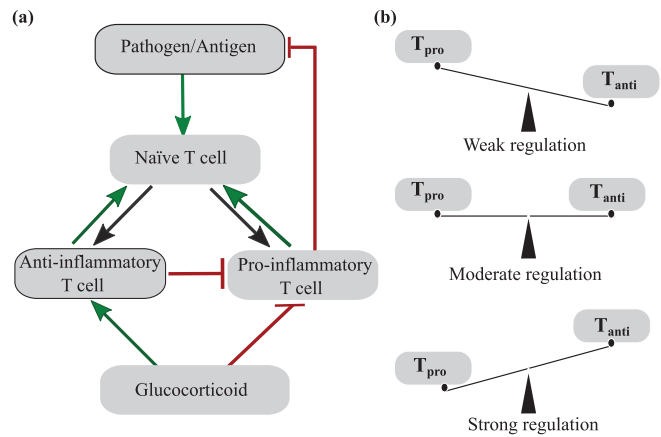


FIG. 1. Coarse-grained model of the adaptive immune response in the presence of GC. (a) There are five primary elements in our system that include pathogen or self-cell containing the antigen:  $CD4+$  naïve T cell, anti-inflammatory T cell, pro-inflammatory T cell, and glucocorticoid. The overall interaction among these five elements is presented in the network. Perturbation from the pathogen in the body leads to the activation of naïve T cells to mature into pro-inflammatory and anti-inflammatory T cells. Mature pro-inflammatory T cells cause the killing of pathogens or self-cells containing the antigen. Further, the mature pro-inflammatory T cells and anti-inflammatory T cells have a role in the self-regulation process of inducing naïve T cells to produce more of themselves, respectively. To control the overexplosion of pro-inflammatory T cells which is an exaggerated immune response, anti-inflammatory T cells and GC cause downregulation of pro-inflammatory T cells. In the given flowchart, the green arrows stand for the upregulation process, red arrows for the inhibition process, and the black arrow represents conversion processes. (b) It represents the population balance of pro-inflammatory T cell ( $T_{pro}$ ) and anti-inflammatory T cell ( $T_{anti}$ ) across the three regulations: weak ( $T_{pro} > T_{anti}$ ), moderate ( $T_{pro} \sim T_{anti}$ ), and strong ( $T_{pro} < T_{anti}$ ).

and immunosuppressive effects on both innate and adaptive immune responses [18,19]. It has been reported in various experimental findings that GC mediates the inhibition in the maturation process of the dendritic cell (DC) via downregulation of  $CD80/86$ ,  $CD1a$ , MHC class II, and reduced cytokine synthesis, including IL-12 and  $TNF\alpha$  [37,39,41]. In the work of Cook *et al.*, they have reported large-scale depletion of lymphocyte, particularly  $CD4+$  T cells and  $CD8+$  T cells, but a significant increase in the activation and proliferation of regulatory T cell or anti-inflammatory T cell by increasing expression of both Ki67 and ICOS, contributing to their immunosuppressive activity. Moreover, they have also recorded changes in the dendritic cell (DC) subtypes population; a similar phenomenon has also been observed in various other *in vivo* and *in silico* models [18,33,42–44].

In this current study, to understand the immunomodulatory role of steroids, we have taken into consideration synthetic glucocorticoids, dex-mediated immune phase transition of adaptive immune response mainly on the  $CD4+$  cell (pro-inflammatory cells and anti-inflammatory T cells). We have developed an interaction-based kinetic scheme, which is depicted in Fig. 1 to portray the direct and indirect effects of GC on the immune system.

**II. MODEL AND METHOD**

The present kinetic immune-network model is developed based on several early experimental and mathematical model studies. Our immune system is comprised of complex and diverse network modules that accompany many participants in terms of immune system cells, which are strongly coupled with each other resulting in synergistic interaction for the maintenance of a healthy physiological condition [1,2,45]. To understand such complex interactions among different immune cells, pathogens, and also to characterize the immunomodulatory role of glucocorticoid (GC), we need to develop a simple modeling pathway that can be interpreted and explained. To understand the correlation among these different immunological interactions of diverse cell types and pathogens, we have to look carefully at how the cells are coupled and how the immunomodulator affects their overall interaction.

**A. Development of the reaction network model of CD4+ T-cell regulation with and without GC**

After careful filtration of all the essential and most important elements, we develop a simpler and refined correlation among the various elements of the immune system, which is presented in Fig. 1. Once the developed network appears to be simple and effective enough, a system of coupled differential equations is used to model the system.

The important elements considered in our coarse-grained model are the following: (i) pathogen/antigen/self-antigen, (ii) naïve T cell (precursor T cell), (iii) pro-inflammatory T cell, (iv) anti-inflammatory T cell, and (v) synthetic glucocorticoid (dexamethasone).

To create a simple albeit effective model of these CD4+ T cells' regulation and modulation, we perform model analyses based on CD4+ T-cell activation, deactivation, and regulation, following some *in vivo* and *in silico* results discussed below.

(I) We have grouped all the CD4+ T cells which cause inflammation and allergic response by downregulation of pathogens; those CD4+ T cells are tagged as pro-inflammatory T cells, which include Th 1, Th 2, Th 17, Th 9, Th 22, and TFH. On the other hand, we grouped all inflammation suppressing or downregulating the role of pro-inflammatory T cells as anti-inflammatory T cells, which include Th3 and Treg. Both anti-inflammatory T cells and pro-inflammatory T cells are the lineages of CD4+ T cells [10,46–53].

(II) As these immune cells are in continuous interaction and clash with foreign invaders and/or pathogens to maintain a healthy state, we can say that there is a continuous predator-prey tussle between the pro-inflammatory T cell (effector T cell) and the pathogen, the pro-inflammatory T cell being the predator and on the other end the pathogen being the prey [9,54,55].

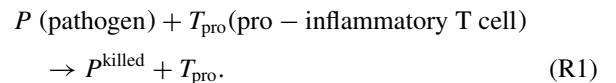
(III) Upon perturbation from pathogens and/or tissue trauma, pattern recognition receptors detect cytokine-induced danger signals. These cytokines induce the production of more of themselves through various biological pathways, which result in the amplification of inflammation. In other words, they play a role in self-activation by inducing naïve T cells to produce more of themselves. This phenomenon has been

observed in various studies where it has been suggested that the pro-inflammatory cytokines produced from mature activated CD4+ T cells induce the production of more of itself through various biological pathways [20,67,68]. The differentiation of naïve cells to mature T cells takes place in the presence of particular cytokines or chemokines; these mature T cells(Th1, Th2, Th17) themselves also produce these cytokines or chemokines(IFN $\gamma$ , IL4, Th17), leading to self-amplification of each of them respectively [56]. From the mathematical model of Jolly and co-workers [57] this self-activation or self-regulation phenomenon is also observed. GC plays a crucial role in such a situation. Being the immunosuppressant, it down-regulates the exaggerated immune response by causing inhibition of many pro-inflammatory cytokines expressions, which includes the granulocyte-macrophage colony-stimulating factor (GM-CSF), interferon- $\gamma$ (IFN $\gamma$ ), TNF, IL-4, IL-5, IL13, IL-9, and IL-17. However, GC also controls the production of cytokine at the post-transcriptional level. It decreases the half-life of TNF mRNA by upregulating tristetraprolin. In this way, GC exerts its anti-inflammatory and immunosuppressive effects on the adaptive immune response. Early studies have reported large-scale depletion of lymphocytes, particularly on CD4+ T cells. However, they have also noted a significant increase in the activation and proliferation of anti-inflammatory T cells by increasing expression, contributing to their immune suppressive activity [18–20,37,42–44,58,59].

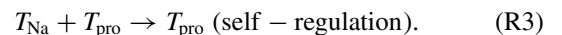
(IV) Glucocorticoid (GC) has a modulatory effect on the population of CD4+ T cells (anti-inflammatory T cells and pro-inflammatory T cells). GC downregulates the pro-inflammatory T cell, i.e., effector T cell population, and on the other hand, it upregulates the anti-inflammatory T-cell population. GC aids in maintaining a perfect balance between these T-cell populations to maintain the homeostasis of the body [20,33].

In the present context, we analyze the following set of biological transformations. Most of them are catalytic reactions in terms of upregulation or downregulation.

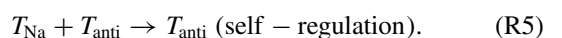
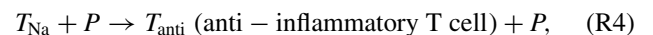
A. The initial step is the elimination of the pathogen by pro-inflammatory T cells,



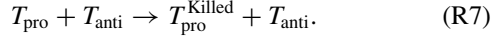
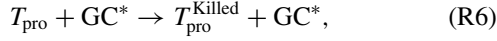
B. Further pathogenic contact and/or pro-inflammatory T-cell contact promotes the maturation of naïve (precursor) T cells into mature pro-inflammatory T cells,



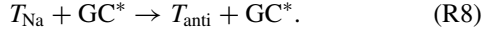
C. Similarly, pathogenic contact and/or anti-inflammatory T-cell contact promote the maturation of naïve (precursor) T cells into mature anti-inflammatory T cells,



D. Both anti-inflammatory T cells and active Glucocorticoid (GC\*) can downregulate the pro-inflammatory T cell either by making pro-inflammatory T cells pathogen insensitive and/or by decreasing the pro-inflammatory T cell count,



E. On the other hand, GC upregulates the production of anti-inflammatory T cells,



## B. Kinetic equations quantifying the reaction network dynamics

Now, some essential additional presumptions we set before writing the kinetic equations:

(i) For pathogen and naïve T cells, each has a birth rate, which contains influx and proliferation rates, and a death rate similar to the decay, which incorporates a scenario of natural cell death. The death rate of all the components is linear with its concentration.

(ii) All the rate parameters are assumed to be constant as obtained from both *in silico* and *in vivo* models and experiments, but it may vary from system to system (i.e., here person to person).

(iii) To scale the unit, here we assume that in the absence of a pathogen, 100 (average number of T cells present in 100 nl of a blood sample) naïve T cells [60] pre-exist, which corresponds to a concentration of 0.000 001 66 nmol/l; an elaborate calculation is described in Appendix B.

(iv) The migration of T cells is assumed to be under the influence of chemotaxis, where the diffusion is much faster in comparison to random cell motility [61]. In order to quantitatively compare the diffusion-controlled rates of T-cell interaction with that of the experimental rates which we have considered in our model, the diffusion-controlled rate constant has been calculated, and a kinetic comparison has also been made. The diffusion-controlled rate calculation has been performed, accounting for the effective diffusion coefficient ( $\sim 67 \mu\text{m}^2/\text{min}$  [62,63]) of CD4+ T cells and its average diameter of  $\sim 10 \mu\text{m}$  [64,65]. It has been observed that the diffusion-controlled rates of T-cell interactions are much faster (rate constant is of the order of  $10^7 \text{nM}^{-1} \text{day}^{-1}$ ) than the experimental rates that we considered in our model. A detailed calculation has been done in Appendix B. However, the range of rate constants for any T-cell mediated bimolecular reactions in our model lies between 0.1 and  $100 \text{nM}^{-1} \text{day}^{-1}$ . Thus, we have ignored the diffusion-controlled rate terms considering the reaction-controlled rates holding the rate-limiting behavior in our kinetic model.

The above recombination, annihilation, and catalytic reactions lead to the following set of coupled equations. The equations are size extensive. However, the size extensibility is the critical robustness of our model. Here, we have employed a deterministic approach; that is, these sets of coupled reaction equations are solved in a deterministic way. It is important to note here that there exists a huge variety of modeling approaches spanning the range of complexity

[3,33,57,63,66–71]. As the present study deals with a complex network of intricate cellular interactions in the immune network perturbed by steroid drugs, in this study, we have adopted a simple reaction-equation-based chemical dynamics approach reducing the complexity scale based on the aforementioned careful assumptions.

## C. Development of two generic models to assess GC-induced reaction network dynamics

In this study, we have modeled the effects of GC on different subsets of immune cells considering two different modes of GC's intake. (i) model I: In this model, along with external administration of GC, we have taken into account natural cellular production GC maintaining its pharmacokinetic characteristics. Here, GC-induced pro-inflammatory T-cell inhibition is linearly dependent on GC concentration following an early treatment [4]. (ii) Model II: GC mediated inhibition was done by applying a saturation function of GC concentration as used by Yakimchuk in a very recent work [33]. Here, one-time external intake of the lower dose of GC and its exponential decay has been considered for comparison purposes.

### 1. Model I

In model I, initially, we have considered a system free of GCs to get a better understanding of the immune response in the absence of any drug. Coupled differential equations for the system in the absence of GCs are shown in Appendix A. Five coupled ODEs of model I in the presence of GC are presented below.

Corresponding five kinetic equations for GC regulation:

$$\frac{dp}{dt} = \sigma_p - k_p T_{\text{pro}} P - m_p P, \quad (1)$$

$$\begin{aligned} \frac{dT_{\text{Na}}}{dt} = & \sigma_{\text{Na}} - k_{rp} T_{\text{Na}} P - k_{ra} T_{\text{Na}} P - k_{\text{pro}} T_{\text{Na}} T_{\text{pro}} \\ & - k_{\text{anti}} T_{\text{Na}} T_{\text{anti}} - k_{aG^*} G^* T_{\text{Na}} - m_{\text{Na}} T_{\text{Na}}, \end{aligned} \quad (2)$$

$$\begin{aligned} \frac{dT_{\text{pro}}}{dt} = & k_{rp} T_{\text{Na}} P + k_{\text{pro}} T_{\text{Na}} T_{\text{pro}} - k_{pa} T_{\text{pro}} T_{\text{anti}} \\ & - k_{pG^*} G^* T_{\text{pro}} - m_{\text{pro}} T_{\text{pro}}, \end{aligned} \quad (3)$$

$$\frac{dT_{\text{anti}}}{dt} = k_{ra} T_{\text{Na}} P + k_{\text{anti}} T_{\text{Na}} T_{\text{anti}} + k_{aG^*} G^* T_{\text{Na}} - m_{\text{anti}} T_{\text{anti}}, \quad (4)$$

$$\frac{dG^*}{dt} = \sigma_{G^*} - k_{\text{abs}} K_b G^* - m_{G^*} G^*. \quad (5)$$

### 2. Model II: Replacing the rate equation of GC by a saturation function

Here, we have followed the method as described by Yakimchuk [33] to reduce the number of coupled differential equations by considering the concentration change of GC with time using a saturation function. Here also, our kinetic scheme is the same as written in the above method part, while only the activated GC concentrations are replaced by a saturation function that takes into account the decay rate of GC. Hence,

GC's pharmacokinetics has not been included here. However, the usage of the saturation function has some limitations. It is restricted only to the lower values of the GC dose so as to capture all three regulation regimes. The following expression  $[1 - \exp(-G^*)]$  tends to 1, with an increase in GC dose that is when  $\exp(-G^*)$  tends to 0. It leaves us with a saturated system. Once it is saturated, a further increase in the GC dose will have a null effect on the overall system.

Glucocorticoid saturation function ( $G$ ):

$$G = k_i(1 - e^{-G^*}), \quad k_i = \text{inhibition rate for a particular immune cell type,}$$

$$G = k_a(1 - e^{-G^*}), \quad k_a = \text{activation rate for a particular immune cell type.}$$

$G^*$  = initial glucocorticoid concentration

Coupled ODE for our system accounting for glucocorticoid concentration as saturation function:

$$\frac{dp}{dt} = \sigma_p - k_p T_{\text{pro}} P - m_p P, \quad (6)$$

$$\begin{aligned} \frac{dT_{\text{Na}}}{dt} = & \sigma_{\text{Na}} - k_{rp} T_{\text{Na}} P - k_{ra} T_{\text{Na}} P - k_{\text{pro}} T_{\text{Na}} T_{\text{pro}} \\ & - k_{\text{anti}} T_{\text{Na}} T_{\text{anti}} - k_{aG^*} (1 - e^{-G^*}) T_{\text{Na}} - m_{\text{Na}} T_{\text{Na}}, \quad (7) \end{aligned}$$

$$\begin{aligned} \frac{dT_{\text{pro}}}{dt} = & k_{rp} T_{\text{Na}} P + k_{\text{pro}} T_{\text{Na}} T_{\text{pro}} - k_{pa} T_{\text{pro}} T_{\text{anti}} \\ & - k_{pG^*} (1 - e^{-G^*}) T_{\text{pro}} - m_{\text{pro}} T_{\text{pro}}, \quad (8) \end{aligned}$$

$$\begin{aligned} \frac{dT_{\text{anti}}}{dt} = & k_{ra} T_{\text{Na}} P + k_{\text{anti}} T_{\text{Na}} T_{\text{anti}} + k_{aG^*} (1 - e^{-G^*}) T_{\text{Na}} \\ & - m_{\text{anti}} T_{\text{anti}}, \quad (9) \end{aligned}$$

$P \rightarrow$  Pathogen,

$T_{\text{Na}} \rightarrow$  naive T cell,

$T_{\text{pro}} \rightarrow$  pro - inflammatory T cell,

$T_{\text{anti}} \rightarrow$  anti - inflammatory T cell,

$G^* \rightarrow$  glucocorticoid.

#### D. Parameter estimation, steady-state, stability, and bifurcation analysis

In order to solve these five coupled differential equations by a deterministic approach, we need to estimate the parameter values associated with these equations. However, the determination of accurate values of all parameters is quite daunting as the rate constants depend on several other factors and differ from one species to another, therefore there is no universality of the rate constants. To overcome this problem, we employ diverse approaches for the determination of the rate constants. For some of the cases in which the rate constant has either been reported in the literature or can be calculated from the literature, we have used that value from the literature. In some cases, where the order of magnitude of the

rate constants has been reported in the literature, that order is taken as the parameter value. The values of parameters taken for solving the coupled differential equations are listed in Table I. Here we have used the same formalism as developed by Fouchet *et al.* to obtain and estimate the parameter values [71].

The concentration of naïve T cells is calculated to be  $1.66 \times 10^{-6}$  nmol/L in the absence of any antigen or pathogen for detailed calculation (see Appendix B). Moreover, these naïve T cells have a turnover of 1% per day. The concentration of the pathogen has also been normalized by setting the birth and death rates of the pathogen to the same value. This is done so that at the steady state, the concentration of the pathogen will be 1. The decay rates of both pro-inflammatory and anti-inflammatory T cells are arbitrarily set to the same value, 0.1, as they account for the proliferation and death rate altogether for both subsets of T cells. So, setting them to the same value leads to mutual compensation, and thus equilibrium is not affected much by their values. Apart from birth rates and death rates, other rate constants are taken from various literature [33,71–74], whose detailed estimations are explained in Appendix B, which also includes related pharmacokinetic rates of glucocorticoid (dex).

We have also done a steady-state and stability analysis of the system. A detailed description is shown in Appendix C.

Bifurcation diagrams were plotted using MATLAB-based software MATCONT to simulate the immune system network of five coupled ODEs of model I in the presence of GC.

#### E. Classification of T-cell regulation

Based on our early study [3,4], we have classified T-cell regulation into the following three groups: (i) weak regulation, where the concentration of pro-inflammatory T cells is very high and the concentration of anti-inflammatory T cells is low, which results in a lowered number of the pathogen; in this phase the immune system is autoimmune prone; (ii) strong regulation, where pro-inflammatory T-cell concentration is low, which is a result of higher concentration of anti-inflammatory T cells leading to high pathogen population; this can be an immunocompromised condition, where our body is prone to disease; and (iii) moderate regulation, where the concentration ratio of pro- and anti-inflammatory T cells is balanced and the immune system holds the characteristics of bistability.

### III. RESULTS AND DISCUSSION

Immunosuppressive drugs are unavoidably correlated with an increased risk of immunocompromised conditions with infection and malignancy. Several studies reported that GC concentration is directly proportional to the growth and enhancement of anti-inflammatory T-cell populations, and alongside, GC suppresses pro-inflammatory T cells. Thus, the dynamics of T-cell populations are very sensitive to the dose of GC [4,37,42,75,76]. Hence, an optimal level of GC administration is essential for the proper functioning of the human body.

Our immune system is a dynamic network encompassing numerous events with a parameter space that may vary from individual to individual. We have accounted for these

TABLE I. Basic parameter values (\*time duration is taken as days).

Si No.	Parameter	Symbol	Value	Units
1	Reproduction rate of pathogen	$\sigma_p$	1	nM/day
2	Rate of pathogen killing by pro-inflammatory T cells	$k_p$	$10^2$	1/(nM day)
3	Death rate of pathogen	$m_p$	1	1/day
4	Birth rate of naïve T cell	$\sigma_{Na}$	1	nM/day
	Death rate of naïve T cell	$m_{Na}$	0.01	1/day
6	Rate of differentiation of naïve T cell to pro-inflammatory T cell which is induced by pathogen	$k_{rp}$	1.01	1/(nM day)
7	Rate of differentiation of naïve T cell to pro-inflammatory T cell which is induced by pro-inflammatory T cell itself (auto catalytic)	$k_{pro}$	variable	1/(nM day)
8	Rate of differentiation of naïve T cell to anti-inflammatory T cell which is induced by anti-inflammatory T cell itself (autocatalytic)	$k_{anti}$	$10^{-1}$	1/(nM day)
9	Rate of differentiation of naïve T cell to anti-inflammatory T cell which is induced by pathogen	$k_{ra}$	1.01	1/(nM day)
10	Rate of inhibition of pro-inflammatory T cell by anti-inflammatory T cell	$k_{pa}$	$10^2$	1/(nM day)
11	Rate of decay of pro-inflammatory T cell	$m_{pro}$	0.1	1/day
12	Rate of decay of anti-inflammatory T cell	$m_{anti}$	0.1	1/day
13	Production rate of glucocorticoid	$\sigma_{G*}$	1.872	nM/day
14	Rate of inhibition of pro-inflammatory T cell by active Glucocorticoid (dex)	$k_{pG*}$	0.57	1/(nM day)
15	Rate of anti-inflammatory T-cell reactivation by active glucocorticoid (dex)	$k_{aG*}$	1.0483	1/(nM day)
16	Absorption rate of glucocorticoid (dex)	$k_{abs}$	102.857	1/day
17	Bioavailability of glucocorticoid (dex)	$k_b$	0.75	unitless
18	Rate of decay of glucocorticoid (dex)	$m_{G*}$	0.415	1/day

events through coupled kinetic rate equations where we have included the values of rate constants and initial pre-existing concentrations of naïve T-cells and GC concentrations as initial inputs. In some instances, a rate constant or a set of rate constants may show higher sensitivity and variability compared to other rate constants. This can be considered as a person-based diversity in the immune system. Thus, we are also interested in exploring sensitive rate parameter(s) and how different sets of parameters control the immune response to the invasion by antigens, including dose dependence of GC.

#### A. GC treated and untreated CD4+ T-cell dynamics and different dynamical phases

We consider a system both with and without GC treatment. By solving the above-mentioned five coupled differential equations of model I, we find the dynamical behavior of pro-inflammatory and anti-inflammatory T cells throughout their course of time evolution, as depicted in Fig. 2, in the presence of GC. In the absence of GC, we have only four coupled rate equations described in Appendix A, and the corresponding dynamical behavior of T cells are shown in Fig. S1 of the Supplemental Material [77]. As several early clinical studies reported that immunosuppressive drugs like GC often leave a long-term effect even long after the treatment has stopped [34–36], in this study, we monitor GC-treated and untreated T-cell dynamics over almost a year-long period. In both cases, after observing the long-term time-evolution of T cells under a small pathogenic perturbation limit, we identify different dynamical phases of T cells and thus classified

majorly into three periods or phases: the expansion period (lag and log phase), the latent period (intermediate stationary phase), and finally, a long-term steady-state as shown in Fig. 2. Similar dynamical phases in terms of lag, log, and intermediate stationary states are well known in the time evolution of microbial growth patterns found in various experimental studies [28,30]. However, in T-cell dynamics studies, this unique *presteady state stationary phase* behavior sustaining for a few months long periods in the intermediate time progression range has not been characterized in any early work. Long-time dependent T-cell regulation studies are limited [3,31,32].

In this stationary phase, the pro-inflammatory and anti-inflammatory T cells maintain highly balanced concentrations and a very small amount of pathogens are observed to be present, which are not likely to cause any disease-related disorder, as shown in Fig. S2. In clinical terminology, it is considered an asymptomatic phase and the phase duration a clinical latent period. A similar latent period is observed in the case of various HIV-based models [31,32] containing a period of clinical latency where the patient does not exhibit any symptoms. Finally, at a longer time, the system reaches a steady state with a higher number of anti-inflammatory T cells and a lower number of pro-inflammatory T cells in the postlatent period depicting the antagonistic nature of pro-inflammatory T cells and anti-inflammatory T cells.

In connection to the early time evolution study of CD4+ T cell [78], here also we find that the initial phase of pro-inflammatory T-cell time evolution has three subphases: expansion, contraction, and memory. The pro-inflammatory T cells clonally increase in number during the first phase,

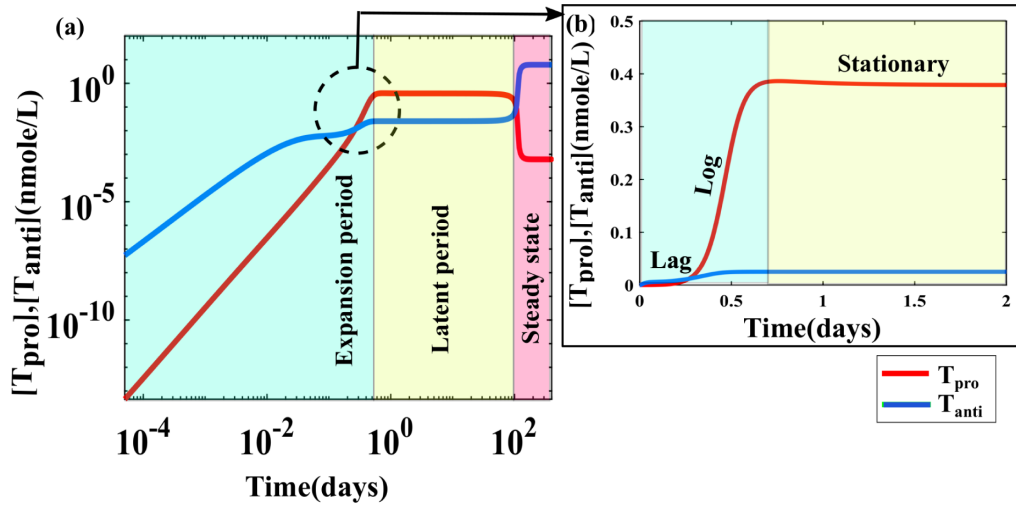


FIG. 2. Time evolution of the immune response of CD4+ T cells in the presence of GC. (a) The log-log plot represents a regime of the immune phase regulation that contains an expansion period, followed by a latent period, i.e., the time range within which the concentration of pro-inflammatory T cells and anti-inflammatory T cells does not change with time. After the latent period, there is a jump to the final steady-state condition. (b) Moreover, the schematic illustration of the phases of immune response mediated by antigen-specific pro-inflammatory T cells is depicted on the left side, where three phases of the initial T cells immune response (lag phase, log phase, and stationary or latent period) are indicated. The time evolution of pro-inflammatory T cells and anti-inflammatory T cells is plotted by solving the coupled kinetic equations using a deterministic approach. In the plot, pro-inflammatory T cells and anti-inflammatory T cells are represented by the red line and the blue line, respectively. The cyan shaded region represents the expansion period, the yellow shaded region represents the latent period, and the pink shaded region represents the steady state. Note that here we consider  $k_{pro} = 56$ , and the other rate values are the same as given in Table I. Note the zoomed portion of (a) is shown in (b).

in the presence of an antigen. Soon after the pathogen load drops down, the contraction phase follows, and the number of pro-inflammatory T cells reduces due to apoptosis. After the contraction phase, the number of pro-inflammatory T cells stabilizes and is maintained for significant periods, representing the memory phase, as depicted in Fig. S3 of the Supplemental Material. Three similar phases have also been reported in other studies [78]. It represents the region of stabilization of CD4+ T cells, where the CD4+ T-cell count stays constant for a certain amount of duration, which also can be referred to as the decision-making phase where the final fate (final steady state) of T cell is being determined. In the presence of pathogenic stimulation, the pro-inflammatory T-cell population will increase after the stationary phase because of the presence of memory T cells. So, the stationary phase has also been referred to as the memory phase [78].

**B. Effect of glucocorticoid on CD4+ T-cell population: Transition from weak to moderate to strong regulation**

Mature pro-inflammatory T cells are the ones responsible for the elimination of pathogen or malignant self-cells [7,9,79]. However, these pro-inflammatory T cells have a role in the self-regulation process of inducing naïve T cells to produce more of themselves. This phenomenon is evident from various studies where it has been suggested that the pro-inflammatory cytokines produced from mature activated CD4+ T cells induce the production of more of themselves through various biological pathways [20,56,80]; this over-amplification of inflammation may lead to an autoimmune

disorder. In various model studies, it has been reported that the anti-inflammatory T cells maintain a balanced regulation of the immune system [3,4,33,71]. Moreover, numerous clinical and experimental studies suggest that the immunomodulatory role of GC causes downregulation of the pro-inflammatory T-cell population to keep it under control [15]. To observe the role of GC in the interaction network of the immune system, we introduce GC-related rate constants and initial pre-existing GC concentration into our system of consideration. After the introduction of GC, we observed that GC has the potential to modulate the immune system from weak regulation to moderate regulation to strong regulation. Along with GC, we have found another sensitive rate constant  $k_{pro}$ , (autocatalytic rate of pro-inflammatory T cells), which also has the ability to modulate the immune system across these three regimes both in the presence and absence of GC.

To investigate several GC-associated factors, we have performed a time-evolution analysis of each participating element after perturbation from the pathogen to study their long-time behavior by varying  $k_{pro}$  both in the absence and presence of GC. By solving our system of equations, we have got all three regulation regimes, both in the presence and absence of GC. Figure 3(a) shows that in the absence of GC, the system falls under a weak regulation limit when we fix  $k_{pro} = 50$ . However, In the presence of a standard level of GC, we found weak regulation Fig. 3(b) at  $k_{pro} = 70$ . Figure 3(c) shows a moderate regulation in the absence of GC at  $k_{pro} = 30$ , where the intermediate stationary phase is sustained with a latent period of 20 days. Furthermore, in the presence of GC, we have found a moderate regulation with the stationary

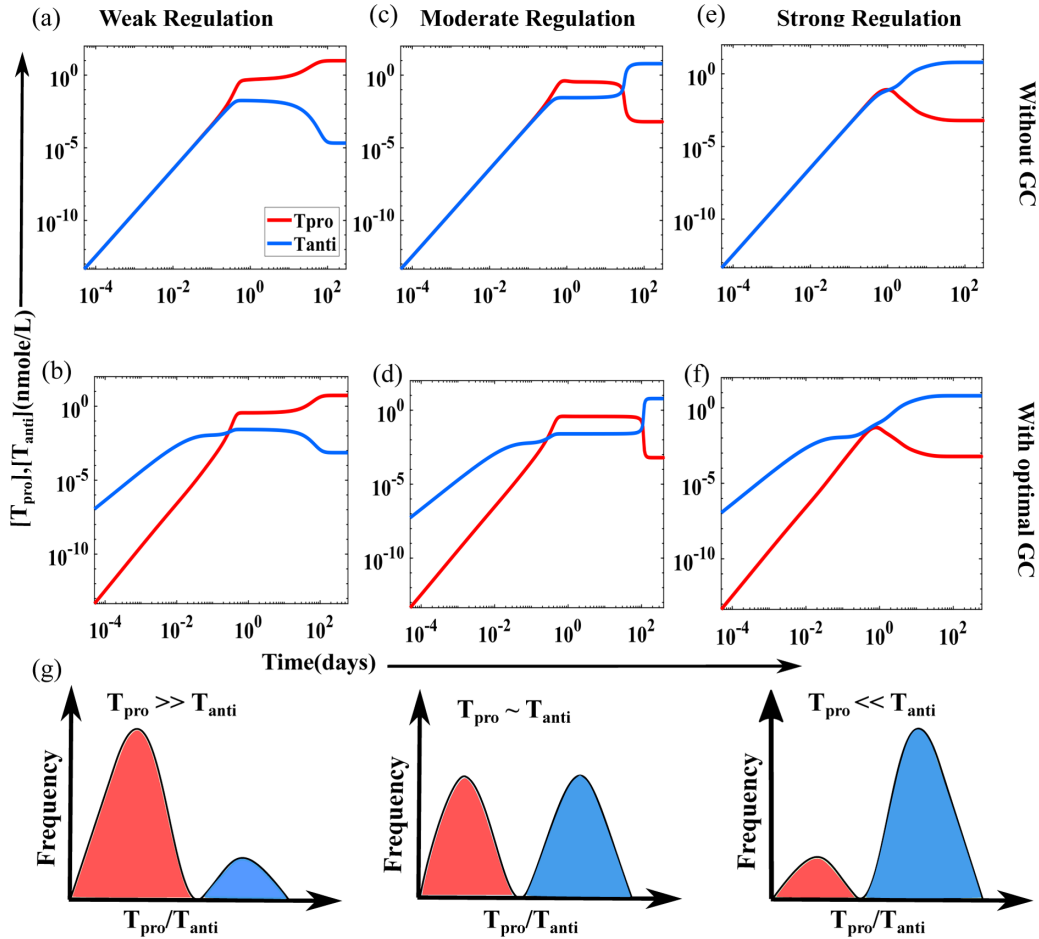


FIG. 3. Time evolution of immune response showing all three regulations, both in the presence and absence of GC. A weak regulation state appears (a) in the absence of GC at  $k_{\text{pro}} = 50$  and (b) in the presence of GC at  $k_{\text{pro}} = 70$ . Moderate regulation state appears (c) in the absence of GC at  $k_{\text{pro}} = 30$ , where the latent period is 20 days. (d) In the presence of GC, moderate regulation appears at  $k_{\text{pro}} = 56$ , where the latent period is 90 days. The system falls into a strongly regulated state at both (e) in the absence of GC and (f) in the presence of GC. The strong regulation remains strong both in the presence and absence of GC at the same value of  $k_{\text{pro}} = 10$ . As we vary  $k_{\text{pro}}$ , other rate parameter values are kept constant and are taken from Table I. A standard dose of dex(GC) is taken to be optimal, which is 38.21 nmol/l ( $\sim 0.75$  mg) [73]. For a detailed explanation for the determination of this optimal value, see Appendix B. In the plot, pro-inflammatory T cells and anti-inflammatory T cells are represented by the red line and the blue line, respectively. (g) We have shown a frequency distribution histogram of pro-inflammatory T cells ( $T_{\text{pro}}$ ) and anti-inflammatory T cells ( $T_{\text{anti}}$ ).

phase extended with a latent period of 90 days at  $k_{\text{pro}} = 56$ , Fig. 3(d). In both cases (absence of GC), as shown in Fig. 3(e) and (presence of GC) Fig. 3(f), we find strong regulation at  $k_{\text{pro}} = 10$ .

However, we find a shift in  $k_{\text{pro}}$ , the parameter value for strong and moderate regulations, when we change our system from the absence of GC to the presence of GC. We find that in the absence of GC, the system is under a strong regulation limit with  $k_{\text{pro}} = 50$ . However, when we introduce GC to our system at  $k_{\text{pro}} = 50$ , we find a moderate regulation which is shown in Fig. S4. The moderate regulation is extended over a wide range of limits, which is shown in Fig. S5. Beyond a certain limit, it falls in a weakly regulated regime. As presented in Fig. 3, The parameter values of  $k_{\text{pro}}$  are very sensitive for determining the strong regulation, moderate regulation, and weak regulation of T cells. Moreover, Fig. 3(g) shows a population distribution of the number ratio between pro- and anti-inflammatory T cells, characterizing the overall classifi-

cation weak, moderate, and strong regulation. This analysis was performed using model I.

### C. Intermediate stationary phase detection at the moderate T-cell regulation limit

Using mode -II, we have replaced GC's rate equation with a saturation function, which presents a one-time external dose intake mode. However, with an increase in the concentration of the GC dose, the saturation function saturates into a constant value. Thus the coupling effect of GC is lost, shown in Fig. S7 of the Supplemental Material. In our model I, we have accounted for the natural metabolism of GC in the fifth rate equation containing all the pharmacokinetic constants. This considers GC's natural recursive regulation, which enables us to get a better understanding of the role of glucocorticoid on T-cell dynamics. Using a rate equation of GC makes our model more robust. We have observed a difference in the dose

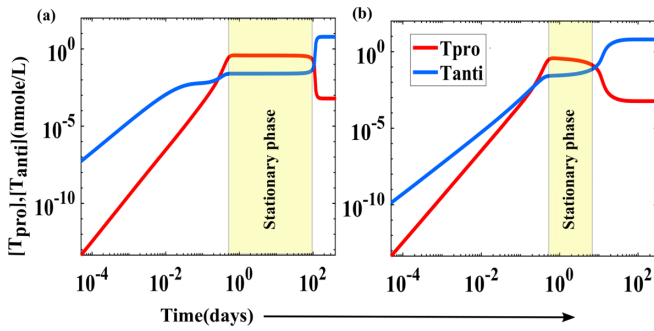


FIG. 4. Time evolution of pro- and anti-inflammatory T cells in the presence of GC. (a) T-cell dynamics from model I, in the presence of standard or optimal concentration of GC = 38.21 nM, (b) one-time external administration using saturation function GC = 0.1 nM ( $\sim 1.96$  micrograms). In the plot, pro-inflammatory T cells and anti-inflammatory T cells are represented by the red line and the blue line, respectively. The yellow shaded region represents the latent period (stationary transition phase). Note that here we consider  $k_{\text{pro}} = 56$ , and the other rate values are the same as given in Table I.

to obtain a moderate regime in models I and II. For capturing the moderate regulation phase using the saturation function, we need to go to the lower values of the GC dose as  $\exp(-G^*)$  tends to zero with the increase in the value of  $G^*$  (dose of dex), which left us with a loss of coupling effect of GC, so while using the saturation function, we are constrained with a lower GC dose. Despite the limitations of this saturation function, we used it for comparison purposes and to make the analysis more comprehensive with an existing model as used by Yakimchuk in a very recent work [33]. However, in both methods, we have distinguished all three regulations: weak, moderate, and strong. Most importantly, the longer-time dynamical analysis of the T-cell population from any of these model studies at their moderate regulation limit consistently demonstrates the existence of an intermediate stationary phase behavior with a significant length of the latent period, as shown in Fig. 4.

#### D. Experimental comparison of dose-dependent T-cell dynamics, understanding glucocorticoid and $k_{\text{pro}}$ -induced stationary phase optimization, and bifurcation phase diagram

To investigate the effect of GC on the T-cell population dynamics, we compare the pro-inflammatory T-cell dynamics data obtained from our model for a short time duration to that of existing experimental and clinical data collected from a cohort of patients suffering from Insulin-dependent diabetes mellitus (IDDM), an autoimmune disease [81]. Our result is in good agreement with the experimental data at a short time scale regime [Figs. 5(a) and 5(b)]. While most of the patient data for autoimmune disease are available for 12–30 days, using our model, we have investigated more extended time-scale dynamics of T cells up to 500 days to understand the long-term phase regulation of T-cell dynamics. In a more profound sense, a long-term effects study can be characterized as “dark data,” where the probability of confronting an unlikely “black swan” type effect increases with time significantly and cannot be ignored. In our case, we have found that upon steroid administration for a prolonged period, the system stays in a near-normal state, which is our stationary

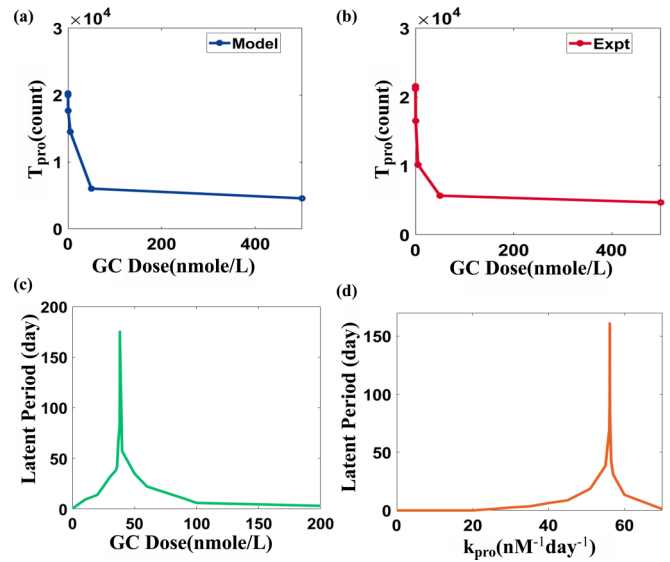


FIG. 5. Evolution of CD4+ pro-inflammatory T cell with a dose of glucocorticoid (dexamethasone) and the sensitivity of the latent period to GC concentration and  $k_{\text{pro}}$ . (a) *In silico* model I showing downregulation of pro-inflammatory T-cell ( $T_{\text{pro}}$ ) with the increase in glucocorticoid dose results in a decrease in pro-inflammatory T cell count. (b) Experimental data collected from insulin-dependent diabetes mellitus (IDDM) in an autoimmune disease patient [81] are in good agreement with our model result. In both cases, the treatment period is considered to be  $\sim 12$ –30 days. (c) Dynamics of the latent period with an increase in the dose of glucocorticoid and (d) dynamics of the latent period with the increase in  $k_{\text{pro}}$  parameter.

phase (90–161 days), Fig. S5. After the stationary phase, the system often switches on a strong regulation limit, an immunocompromised state. Here comes the relevance of a long-term (dark data) dose and time dependence of steroid drug administration. It has precisely captured the pathogenic reactivation (black swan effect), a known outcome of long-term chemotherapies [82–84].

After analyzing CD4+ T-cell dynamics over long-term steroid drug administration for around 500 days, we find that GC has a significant role in efficiently keeping the immune system in a moderate regulation regime for a significantly longer duration. Moreover, it has also been seen that the moderate regime is conserved for a specific range of GC, which we consider an optimal range, as shown in Fig. 5(c). Our findings also show that at a lower value or in the absence of GC, the latent period is small, leading to a risk of autoimmune disease due to the uncontrolled rapid growth of pro-inflammatory T cells (weak regulation). Moreover, when the GC dose is very high, the system again falls in the range of a smaller latent period with a significantly smaller population of pro-inflammatory T cells corresponding to an immune-compromised condition (strong regulation). In between strong and weak regulations, we observe the divergence of the system to a latent period peak, which corresponds to moderate regulation. Our results signify the sensitivity of the immune system to the dose of GC. The optimal range of GC (dex) is in accordance with the experimental finding [73,85] (for a detailed explanation, see Appendix B). In Fig. 5(c) the  $k_{\text{pro}}$  value is taken under a moderate regulation regime,

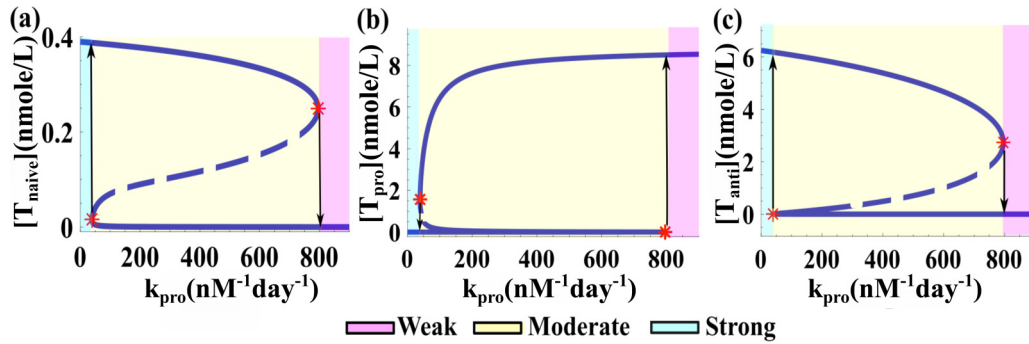


FIG. 6. Bifurcation phase diagram of CD4+ T cell. Bifurcation diagram depicting the changes in (a) naïve T cell, (b) pro-inflammatory T cell, and (c) anti-inflammatory T-cell levels with variations in the levels of bifurcation parameter  $k_{\text{pro}}$ . (b) The highest pro-inflammatory T-cell levels correspond to weak regulation, intermediate levels of pro-inflammatory T cell correspond to a moderate regulation, and lowest levels of pro-inflammatory T cell correspond to strong regulation, as indicated by different colors (Weak, strong and moderate regulations are predefined immune classes as shown by background colors). Stable, steady states are indicated by solid (blue) lines; unstable steady states, by dashed (blue) lines. (c) Since pro-inflammatory T cell and anti-inflammatory T cell have antagonistic behavior, the dynamics of anti-inflammatory T cells are the opposite of pro-inflammatory T cell, high anti-inflammatory T cell corresponds to strong regulation, and low anti-inflammatory T cell corresponds to weak regulation. In all three bifurcation plots, characteristic bistability has been observed, showing the parameter space of monostable and bistable phases characterized over each classified immune regulation regime as colored. Note that all the constant rate values are taken the same as given in Table I. In the plot, naïve T cell ( $T_{\text{naive}}$ ), pro-inflammatory T cells ( $T_{\text{pro}}$ ), and anti-inflammatory T cells ( $T_{\text{anti}}$ ) are taken in nM concentration.

and all other parameters and rate constants are taken from Table I.

We have also looked into the sensitivity of the latent period with respect to the change of a sensitive rate constant  $k_{\text{pro}}$ , which is represented in Fig. 5(d). At a specific range of  $k_{\text{pro}}$  value, the immune system is in a moderate regulation with a large latent period. We have observed this at both lower and higher values of  $k_{\text{pro}}$ . The latent period is small, showing strong regulation and weak regulation, respectively. By changing the  $k_{\text{pro}}$  values, we have modulated the system from strong regulation to moderate regulation to weak regulation. At  $k_{\text{pro}} = 56.146$ , the system is at moderate regulation and has the largest range of latent period, and at  $k_{\text{pro}} = 56.147$ , the system converts from moderate regulation to weak regulation, with a significant decrease in the latent period. This accounts for the sensitivity of the  $k_{\text{pro}}$  value for its response in the latent period of immune system regulation. As  $k_{\text{pro}}$  can vary from person to person, we have taken varied values of  $k_{\text{pro}}$  and determined the latent period, and all other parameters and rate constants are taken from Table I; the dose of GC (dex) is taken to be optimal, which is 38.21 nmol/L—the determination of this optimal value is explained in detail in Appendix B.

As discussed above, the latent period is a very sensitive response parameter to both GC and  $k_{\text{pro}}$ , and with a change in the value of  $k_{\text{pro}}$  or GC, we can observe a shift of the system's regimes. However, our system in the presence of optimal doses of glucocorticoid shows the conservation of moderate regulation for large limits of  $k_{\text{pro}}$  and GC dose shown in Figs. S5 and S6, respectively, in the Supplemental Material. As shown in Fig. 5, the latent period keeps increasing slowly, then there is sudden divergence, and it falls, modulating the system across weak to moderate to strong regulation limits. The modulation of the latent period when it decreases can be an early warning signal of abrupt change in dynamics of the system from one stable state (moderate regulation) to another

(weak regulation) upon small perturbation like small change in the GC dose or a sensitive rate parameter like  $k_{\text{pro}}$  values.

With the classification of three regulation regions (weak, moderate, strong) we have investigated the boundaries between any two phases in the immune phase space accounting for the above-mentioned two sensitive order parameters:  $k_{\text{pro}}$  and [GC]. The immune phase diagram is shown in Fig. S8. In light of our previous studies [3,4], it is worth mentioning here that distinguishing bistability in the moderate regulation regime is a key concept for understanding the basic phenomena of pro- and anti-inflammatory T-cell regulation. All these phenomena arise due to the nonlinearity of the biological system [86–88]. The phase diagram presented in Fig. S8 depicts the normalized concentration of pro-inflammatory T cells with respect to total CD4+ T-cell concentration (sum of pro- and anti-inflammatory T cells) as a function of both  $k_{\text{pro}}$  and [GC]. It is plotted using numerical results from the solution of our system of equations obtained from model 1. In this immune phase diagram, the bistable or moderate regulation regime is a narrow constricted region. However, we find this only near bistable regions; the immune system is sensitive to GC. At too weak or strong regulation, the system loses its GC sensitivity. It suggests that when a person is close to a moderate regime of parameter space, then only a synthetic GC intake may help.

To further characterize the parameter space for the possible coexistence of states (bistability), we analyze bifurcation diagrams for multiple parameter sets and also the parameter set mentioned in Table I. The rate constant  $k_{\text{pro}}$  is chosen as a bifurcation parameter. To mention again,  $k_{\text{pro}}$  is the rate of differentiation of naïve T cell to pro-inflammatory T cell, which is induced by the pro-inflammatory T cell itself, a self-activation-like phenomenon. We find that the system holds characteristic bistability within a certain range of  $k_{\text{pro}}$ , as shown in Fig. 6. This bistable region is separated by two monostable regions.

#### IV. CONCLUSION

While the steroid hormone glucocorticoid (GC) is extensively used to control many acute and chronic inflammatory disorders, it is well documented that GC can cause a wide array of adverse effects that are both dose and time dependent. Both the higher doses and long-term usage of low to moderate GC doses increase the risk of life-threatening infections due to the immunological cytokine imbalance and many associated factors [16,35,75,89,90]. While it is absolutely necessary to understand the immune responses of the T lymphocytes systematically, in a dose and time-dependent manner, clinically, it is a daunting task. However, a simple chemical dynamic model comprised of GC-mediated cellular-level interactions among different subsets of T cells and preliminary clinical guidance over a known interaction-level database and parameters can provide valuable information about the state of our body. These approaches are often amenable to clinical measurements and certain conclusions. Thus, understanding the immune response of the complex human system requires collaboration between physicists, chemists, biologists, and clinical scientists. In particular, one may need to borrow the mathematical models and concepts from physics and combine certain rules of chemistry to understand the complex biological processes and interactions. There have been notable efforts in this interdisciplinary direction, although a lot remains to be achieved.

Below we summarized the key highlights of this study:

(i) To monitor both time and dose-dependent GC effects on T-cell dynamics, we have developed two independent mathematical models. The first model considers the pharmacokinetic characteristics of GC, and in the other model, a saturation function is used to capture GC's dose dependence of T-cell regulation. Both the models unanimously provide a similar dynamical pattern of pro- and anti-inflammatory T cells.

(ii) In this long-term CD4+ T-cell kinetic study, three characteristic dynamic phases have been distinguished: growth (lag and log), the stationary or latent period, and the long-term-steady or memory phase. These phases are analogous to the growth kinetics of microbial cells.

(iii) In this study, depending on the population ratio between the pro- and anti-inflammatory T cells, we have quantitatively distinguished three classes of immune regulations: strong, weak, and moderate both in the presence and absence of steroid hormone GC.

(iv) A characteristic intermediate "stationary phase" is detected to develop especially in the moderate regulation limit under the influence of pathogen. This is an apparent near-normal clinically asymptomatic or latent phase, and the corresponding latent period can be sustained for a long time (more than a couple of months), where the pathogenic load drops dramatically. The emergence of prolonged clinical latency correlates well with the CD4+ T-cell dynamics that have been monitored in the case of HIV infection [32].

(v) GC dose dependence of the pro-inflammatory T-cell population obtained from our model for a short time duration correlates well with the existing experimental data collected from insulin-dependent diabetes mellitus (IDDM) in an autoimmune disease patient [81]. The GC dose-dependent T-cell

downregulation curve shows that the transition midpoint ranges 5–40 nmol/L, close to an optimal GC dose ( $\sim 38.21$  nmol/L). We also find the latent period in the intermediate stationary phase to vary nonmonotonically as a function of GC dose. At a standard or optimal level of GC concentration, the latent period is found to reach the peak implying that GC optimizes the stationary phase by subtly balancing the population ratio between the pro- and anti-inflammatory T cell. However, this needs to be clinically verified.

(vi) At a longer time, after the asymptomatic phase, a long-term steady-state outcome is reached, which is a decision-making phase of the system. In this decision-making phase, the system either deactivates or reactivates the pro-inflammatory actions, which decides the fate of the antigen or disease. In the presence of steroid administration, after a prolonged stationary phase, the system has a general tendency to switch on a strong regulation limit where immunity is challenged. In a broader sense, such long-term steroid effects are characterized as dark data where the probability of encountering a black swan type effect increases with time significantly and cannot be ignored [74–76]. And, here comes the relevance of dose and time dependence of steroid drug administration. It is now well known that in addition to GC, many other immunosuppressive drugs such as prednisone, pain killers (morphine, codeine, hydrocodone, opioids), and other chemotherapeutic drugs perform life-saving tasks within the human body but often cause pathogen or viral reactivation when immunity is critically suppressed. In fact, during chemotherapy, a viral reactivation event is very real [82–84].

(vii) Finally, understanding the final steady-state outcome in different immune regulation limits and their coexistence is illustrated by an immune phase diagram which reveals that the steroid-dependent moderate or healthy phase is a constricted immune regime that is adept at tolerating a wide range of pathogenic stimuli when the autocatalytic rate of pro-inflammation is low (i.e., when T cells are less aggressive). From the bifurcation diagram, we get characteristic bistability when  $k_{\text{pro}}$  was chosen to be a bifurcation parameter for multiple parameter sets.

While the immunosuppressive drug GC potentially controls weak or autoimmune-prone T-cell regulation, the study reveals an odd characteristic of steroid-dependent T-cell dynamics, which highlights a prolonged stationary phase. In the stationary phase, while the system is autoimmune controlled under the steroid treatment, it is now more vulnerable to pathogen reactivation. These challenges can be circumvented by long-term diagnostic measures, especially to monitor the prolonged latency in the intermediate stationary phase and by prescribing antiviral treatment along with GC treatment in an effort to ward off pathogen reactivation, as suggested by a few clinical studies [32,91,92]. Our study indeed provides the rationale behind such modes of treatment and encourages awareness against imprudent steroid medication.

In this study, we have employed a simple chemical network model of the immune system to understand the effect of steroid drugs like GC. This eventually results in an optimized stationary phase to control autoimmune disorders without any adverse effect at least for some time (if not longer). The non-monotonic steroid dependence of the intermediate stationary phase can be used as a diagnostic marker for steroid treatment,

especially when the system loses bistability. In the future, we shall attempt to explore more towards the noise-induced bistability and fluctuation-driven immune response to monitor how the fluctuation of certain T-cell subsets affects the stationary phase latency and steady-state outcome during steroid treatment.

The data that support the findings of this study are available in the main text and Supplemental Material but are also available from the corresponding author upon request.

### ACKNOWLEDGMENTS

This work was supported in part by start-up grants from IISER Kolkata. S.R. acknowledges support from the Department of Biotechnology (DBT) (Grant No. BT/12/IYBA/2019/12) and Science and Engineering Research Board (SERB), Department of Science and Technology (DST), Govt. of India (Grant No. SRG/2020/001295).

### APPENDIX A: SIMULATIONS IN THE ABSENCE OF GLUCOCORTICOID

In order to look at the dynamics of the system in the absence of glucocorticoids we remove all the terms involving the glucocorticoids. Hence, we would have four coupled ODEs, as given below.

Coupled ODEs for the system in the absence of glucocorticoid (representing drug-free immune regulation):

$$\frac{dp}{dt} = \sigma_p - k_p T_{\text{pro}} P - m_p P, \quad (\text{A1})$$

$$\begin{aligned} \frac{dT_{\text{Na}}}{dt} = & \sigma_{\text{Na}} - k_{rp} T_{\text{Na}} P - k_{ra} T_{\text{Na}} P - k_{\text{pro}} T_{\text{Na}} T_{\text{pro}} \\ & - k_{\text{anti}} T_{\text{Na}} T_{\text{anti}} - m_{\text{Na}} T_{\text{Na}}, \end{aligned} \quad (\text{A2})$$

$$\frac{dT_{\text{pro}}}{dt} = k_{rp} T_{\text{Na}} P + k_{\text{pro}} T_{\text{Na}} T_{\text{pro}} - k_{pa} T_{\text{pro}} T_{\text{anti}} - m_{\text{pro}} T_{\text{pro}}, \quad (\text{A3})$$

$$\frac{dT_{\text{anti}}}{dt} = k_{ra} T_{\text{Na}} P + k_{\text{anti}} T_{\text{Na}} T_{\text{anti}} - m_{\text{anti}} T_{\text{anti}}. \quad (\text{A4})$$

### APPENDIX B: PARAMETER ESTIMATION AND OTHER CALCULATIONS

#### 1. Calculation of T-cell diffusion-limited rate constant

The diameter of T cell has been taken to be  $10 \mu\text{m}$  [64,65], and the effective diffusion coefficient is taken to be  $\sim 67 \mu\text{m}^2/\text{min}$  [62].

The T-cell diffusion-limited rate constant  $k_{\text{Diff}} = 4\pi N_A (r_A + r_B)(D_A + D_B)$  [93], where  $r$  and  $D$  represent the radius and the diffusion coefficient of T cells, respectively.  $N_A$  is Avogadro's number. From the above formula,  $k_{\text{Diff}}$  was calculated to be  $1.46 \times 10^7 \text{ nM}^{-1} \text{ day}^{-1}$

#### 2. Determination of initial naïve T-cell concentration

We have assumed that in the absence of an antigen, 100 CD4+ naïve T cells can pre-exist within this fixed volume (100 nl) [4,60],

$$6.022 \times 10^{23} \text{ naïve T cell} \rightarrow 1 \text{ mole},$$

$$100 \text{ naïve T cell} \rightarrow 1.6605 \times 10^{-13} \text{ nmole},$$

$$\begin{aligned} \text{Concentration} &= \frac{n}{v} \\ &= \frac{1.6605 \times 10^{-13} \text{ nmole}}{100 \text{ nl}} \\ &= 1.66 \times 10^{-6} \text{ nmole/l}. \end{aligned}$$

#### 3. Determination of GC dose

The dose of dexamethasone at which it shows its immunomodulatory activity is 0.75 mg [73,85]. The volume distribution of dexamethasone is 40–60 l [73,85],

$$\text{Concentration of GC (dex)} = \frac{\text{dose}}{\text{volume distribution (VD)}},$$

$$\text{VD for dex} = \frac{\text{clearance}}{\text{elimination rate}} = 40\text{--}60 \text{ L} \sim 50 \text{ l},$$

$$\begin{aligned} \text{Concentration of GC (dex)} &= \frac{0.75 \text{ mg}}{50 \text{ l}} \\ &= \frac{1910.978 \text{ nmole}}{50 \text{ L}} \\ &= 38.21 \text{ nmole/l s}. \end{aligned}$$

#### 4. Parameter estimation

In the work of Fouchet *et al.*, they have considered APC activation by antigens, effector T cells, and regulatory T cells to be variable [71]. However, in their work they have considered the maturation of naïve T-cell via the pathway of APC to be 1. In our work, we have considered maturation rate of naïve T cell value ranging from 0.1-1.01 presented in Table I, based on our early study [3,4], as the antigen of the invaded pathogen or self-antigen leads to activation of resting APC and active APC, which further leads to activation of the maturation process of naïve T cells into pro-inflammatory T cells and anti-inflammatory T cells, from which we can conclude that the antigen-induced rate of differentiation of naïve T cell to the pro-inflammatory and anti-inflammatory T cell can be the sum of APC activation by antigens and naïve T-cell maturation rate activated by APC. However, the glucocorticoid related pharmacokinetic rate constants are taken from various literature [72,73,85,94,95]:

$$\text{absorption rate of glucocorticoid (dex) [73]} = 4.8729 \pm 8.4998 \text{ 1/h},$$

$$\text{bioavailability of glucocorticoid (dex) [72]} = 70\text{--}78\% (75\%)$$

$$\text{biological half life of glucocorticoid (dex) [73]} = 36\text{--}72 \text{ h} (40 \text{ h})$$

rate of decay of glucocorticoid (dex) =  $m_{G^*}$ ,

$$m_{G^*} = \frac{\ln[2]}{\text{biological half - life}} = \frac{\ln[2]}{40 \text{ h}} = \frac{\ln [2]}{40} (24) \text{ day}^{-1} = 0.4158 \text{ day}^{-1}.$$

**APPENDIX C: STEADY-STATE AND STABILITY ANALYSIS**

For the system to be in a steady state, it should have the following conditions:

$$\frac{dP}{dt} = \frac{dT_{Na}}{dt} = \frac{dT_{pro}}{dt} = \frac{dT_{anti}}{dt} = \frac{dG^*}{dt} = 0, \tag{C1}$$

$$P = \frac{\sigma_p}{k_p T_{pro} + m_p}, \tag{C2}$$

$$T_{Na} = \frac{\sigma_{Na}}{(k_{rp}P + k_{ra}P + k_{pro}T_{pro} + k_{anti}T_{anti} + k_{aG^*}G^* + m_{Na})}, \tag{C3}$$

$$T_{pro} = \frac{k_{rp}T_{Na}P}{(-k_{pro}T_{Na} + k_{pa}T_{anti} + k_{pG^*}G^* + m_{pro})}, \tag{C4}$$

$$T_{anti} = \frac{k_{ra}T_{Na}P + k_{aG^*}G^*T_{Na}}{(-k_{anti}T_{Na} + m_{anti})}, \tag{C5}$$

$$G^* = \frac{\sigma_{G^*}}{(k_{abs}K_b + m_{G^*})}. \tag{C6}$$

The latent period and steady state found from our MATLAB plot satisfy these steady-state conditions.

The Jacobian matrix for the given system of ODEs (1)–(5) is represented as follows:

$$\begin{pmatrix} -k_p T_{pro} - m_p & 0 & 0 & 0 & 0 \\ -k_{rp} T_{Na} - k_{ra} T_{Na} & -(k_{rp} P + k_{ra} P + k_{pro} T_{pro} + k_{anti} T_{anti} + k_{aG^*} G^* + m_{Na}) & -k_p P & 0 & 0 \\ k_{rp} T_{Na} & k_{rp} P + k_{pro} T_{pro} & -k_{pro} T_{Na} & -k_{anti} T_{Na} & -k_{aG^*} T_{Na} \\ k_{ra} T_{Na} & k_{ra} P + k_{anti} T_{anti} + k_{aG^*} G^* & k_{pro} T_{Na} - k_{pa} T_{anti} - k_{pG^*} G^* - m_{pro} & -k_{pa} T_{pro} & -k_{pG^*} T_{pro} \\ 0 & 0 & 0 & k_{anti} T_{Na} - m_{anti} & k_{aG^*} T_{Na} \\ & & & 0 & -k_{abs} K_b - m_{G^*} \end{pmatrix}$$

To analyze the steady-state conditions when there are no source parameters, there is an equilibrium point when all the concentration of all the elements is equal to zero:  $(P, T_{Na}, T_{pro}, T_{anti}, G^*) = (0, 0, 0, 0, 0)$ . Then the Jacobean matrix is presented as follows:

$$\begin{pmatrix} -m_p & 0 & 0 & 0 & 0 \\ 0 & -m_{Na} & 0 & 0 & 0 \\ 0 & 0 & -m_{pro} & 0 & 0 \\ 0 & 0 & 0 & -m_{anti} & 0 \\ 0 & 0 & 0 & 0 & -k_{abs} K_b - m_{G^*} \end{pmatrix}$$

Then the eigenvalues of the Jacobean matrix are  $-m_p, -m_{Na}, -m_{pro}, -m_{anti}, -k_{abs}K_b - m_{G^*}$ , since all the rate constants considered in the system are positive. We conclude that the five eigenvalues of the system is negative, which justifies the stability of the considered system.

The saturation point for the respective ODEs when we consider each ODE is mutually exclusive.

From Eq. (C2)  $P$  will saturate at

$$P = \frac{\sigma_p}{m_p} \text{ (in absence of } T_{Na}, T_{pro}, T_{anti}, G^* \text{)}.$$

From Eq. (C3)  $T_{Na}$  will saturate at

$$T_{Na} = \frac{\sigma_{Na}}{m_{Na}} \text{ (in absence of } P, T_{pro}, T_{anti}, G^* \text{)}.$$

From Eq. (C4)  $T_{pro}$  will saturate at

$$T_{pro} = 0 \text{ (in absence of } P, T_{Na}, T_{anti}, G^* \text{)}.$$

From Eq. (C5)  $T_{anti}$  will saturate at

$$T_{anti} = 0 \text{ (in absence of } P, T_{Na}, T_{pro}, G^* \text{)}.$$

From Eq. (C6)  $G^*$  will saturate at

$$G^* = \frac{\sigma_{G^*}}{(k_{\text{abs}}K_b + m_{G^*})} \text{ (in absence of } P, T_{\text{Na}}, T_{\text{pro}}, T_{\text{anti}}).$$

- 
- [1] A. S. Perelson, Immune network theory, *Immunological Reviews* **110**, 5 (1989).
- [2] N. K. Jerne, Towards a network theory of the immune system, *Ann. Immunol. (Paris)* **125C**, 373 (1974).
- [3] S. Roy and B. Bagchi, Fluctuation theory of immune response: A statistical mechanical approach to understand pathogen induced T-cell population dynamics, *J. Chem. Phys.* **153**, 45107 (2020).
- [4] S. Roy, K. Shrinivas, and B. Bagchi, A stochastic chemical dynamic approach to correlate autoimmunity and optimal vitamin-D range, *PLoS ONE* **9**, e100635 (2014).
- [5] D. A. Smith and D. R. Germolec, Introduction to immunology and autoimmunity, *Environmental Health Perspectives* **107 Suppl**, 661 (1999).
- [6] D. E. Jones and A. G. Diamond, The basis of autoimmunity: An overview, *Baillieres. Clin. Endocrinol. Metab.* **9**, 1 (1995).
- [7] D. D. Chaplin, Overview of the immune response, *J. Allergy Clin. Immunol.* **125**, S3 (2010).
- [8] C. Janeway, *Immunobiology: The Immune System in Health and Disease* (Current Biology Publications, 1999).
- [9] B. Alberts, A. Johnson, J. Lewis, M. Raff, K. Roberts, and P. Walter, *Molecular Biology of the Cell*, 4th ed. (Garland Science, New York, 2002).
- [10] S. Sakaguchi and N. Sakaguchi, Regulatory T cells in immunologic self-tolerance and autoimmune disease, *Int. Rev. Immunol.* **24**, 211 (2005).
- [11] K. Orihara, S. Nakae, R. Pawankar, and H. Saito, Role of regulatory and proinflammatory T-cell populations in allergic diseases, *World Allergy Organ. J.* **1**, 9 (2008).
- [12] M. Hewison, Vitamin D and innate and adaptive immunity, *Vitam. Horm.* **86**, 23 (2011).
- [13] M. Hewison, An update on vitamin D and human immunity, *Clin. Endocrinol. (Oxf)* **76**, 315 (2012).
- [14] M. Cutolo, C. Pizzorni, and A. Sulli, Vitamin D endocrine system involvement in autoimmune rheumatic diseases, *Autoimmun. Rev.* **11**, 84 (2011).
- [15] M. J. Herold, K. G. McPherson, and H. M. Reichardt, Glucocorticoids in T cell apoptosis and function, *Cell. Mol. Life Sci.* **63**, 60 (2005).
- [16] J. R. Flammer and I. Rogatsky, Minireview: Glucocorticoids in autoimmunity: Unexpected targets and mechanisms, *Mol. Endocrinol.* **25**, 1075 (2011).
- [17] T. E. Davis, K. Kis-Toth, A. Szanto, and G. C. Tsokos, Glucocorticoids suppress T cell function by up-regulating MicroRNA-98, *Arthritis Rheum.* **65**, 1882 (2013).
- [18] U. Baschant and J. Tuckermann, The role of the glucocorticoid receptor in inflammation and immunity, *J. Steroid Biochem. Mol. Biol.* **120**, 69 (2010).
- [19] Y. Chinenov and I. Rogatsky, Glucocorticoids and the innate immune system: Crosstalk with the toll-like receptor signaling network, *Mol. Cell. Endocrinol.* **275**, 30 (2007).
- [20] D. W. Cain and J. A. Cidlowski, Immune regulation by glucocorticoids, *Nat. Rev. Immunol.* **17**, 233 (2017).
- [21] O. Bereshchenko, S. Bruscoli, and C. Riccardi, Glucocorticoids, sex hormones, and immunity, *Front. Immunol.* **9**, 1332 (2018).
- [22] P. Fang, X. Li, J. Dai, L. Cole, J. A. Camacho, Y. Zhang, Y. Ji, J. Wang, X.-F. Yang, and H. Wang, Immune cell subset differentiation and tissue inflammation, *J. Hematol. Oncol.* **11**, 97 (2018).
- [23] B. Peng, H. Zhang, W. Chen, B. Hou, Z.-J. Qiu, H. Shao, H. Zhu, B. Monserrat, D. Fu, H. Weng, and C. M. Soukoulis, Subpicosecond photo-induced displacive phase transition in two-dimensional MoTe<sub>2</sub>, *npj 2D Mater. Appl.* **4**, 14 (2020).
- [24] P. Papon, J. Leblond, and P. H. E. Meijer, *The Physics of Phase Transitions: Concepts and Applications* (Springer-Verlag, Berlin, Heidelberg, 2002).
- [25] A. Pal, S. Gohil, S. Sengupta, H. Poswal, S. Sharma, S. Ghosh, and P. Ayyub, Structural phase transitions in trigonal selenium induce the formation of a disordered phase, *J. Phys.: Condens. Matter* **27**, 415404 (2015).
- [26] A. Sengupta, S. Sengupta, and G. I. Menon, Driven disordered polymorphic solids: Phases and phase transitions, dynamical coexistence and peak effect anomalies, *Phys. Rev. B* **81**, 144521 (2010).
- [27] F. Demoling, D. Figueroa, and E. Bååth, Comparison of factors limiting bacterial growth in different soils, *Soil Biol. Biochem.* **39**, 2485 (2007).
- [28] L. Wang, D. Fan, W. Chen, and E. M. Terentjev, Bacterial growth, detachment and cell size control on polyethylene terephthalate surfaces, *Sci. Rep.* **5**, 15159 (2015).
- [29] R. Kolter, D. A. Siegle, and A. Tormo, The stationary phase of the bacterial life cycle, *Annu. Rev. Microbiol.* **47**, 855 (1993).
- [30] R. L. Bertrand, Lag phase is a dynamic, organized, adaptive, and evolvable period that prepares bacteria for cell division, *J. Bacteriol.* **201**, e00697 (2019).
- [31] C. Selinger and M. G. Katze, Mathematical models of viral latency, *Curr. Opin. Virol.* **3**, 402 (2013).
- [32] E. Sánchez and E. A. Hernandez-Vargas, in *Modeling and Control of Infectious Diseases in the Host* (Academic Press, 2019), p. 105.
- [33] K. Yakimchuk, Mathematical modeling of immune modulation by glucocorticoids, *Biosystems* **187**, 104066 (2020).
- [34] M. Yasir, A. Goyal, P. Bansal, and S. Sonthalia, *Corticosteroid Adverse Effects* (StatPearls, Treasure Island, FL, 2020).
- [35] I. S. Alan and B. Alan, in *Pharmacokinetics and Adverse Effects of Drugs*, edited by N. Malangu (IntechOpen, Rijeka, 2018).
- [36] M. Ciriaco, P. Ventrice, G. Russo, M. Scicchitano, G. Mazzitello, F. Scicchitano, and E. Russo, Corticosteroid-related central nervous system side effects, *J. Pharmacol. Pharmacother.* **4**, S94 (2013).
- [37] W. J. Aston, D. E. Hope, A. M. Cook, L. Boon, I. Dick, A. K. Nowak, R. A. Lake, and W. J. Lesterhuis, Dexamethasone

- differentially depletes tumour and peripheral blood lymphocytes and can impact the efficacy of chemotherapy/checkpoint blockade combination treatment, *OncoImmunology* **8**, e1641390 (2019).
- [38] A. J. Giles, M.-K. N. D. Hutchinson, H. M. Sonnemann, J. Jung, P. E. Fecci, N. M. Ratnam, W. Zhang, H. Song, R. Bailey, D. Davis, C. M. Reid, D. M. Park, and M. R. Gilbert, Dexamethasone-induced immunosuppression: Mechanisms and implications for immunotherapy, *J. Immunother. Cancer* **6**, 51 (2018).
- [39] I. Szatmari and L. Nagy, Nuclear receptor signalling in dendritic cells connects lipids, the genome and immune function, *EMBO J.* **27**, 2353 (2008).
- [40] D. Liu, A. Ahmet, L. Ward, P. Krishnamoorthy, E. D. Mandelcorn, R. Leigh, J. P. Brown, A. Cohen, and H. Kim, A practical guide to the monitoring and management of the complications of systemic corticosteroid therapy, *Allergy, Asthma, Clin. Immunol.* **9**, 30 (2013).
- [41] L. Freeman, M. Hewison, S. v Hughes, K. N. Evans, D. Hardie, T. K. Means, and R. Chakraverty, Expression of 11beta-hydroxysteroid dehydrogenase type 1 permits regulation of glucocorticoid bioavailability by human dendritic cells, *Blood* **106**, 2042 (2005).
- [42] A. M. Cook, A. M. McDonnell, R. A. Lake, and A. K. Nowak, Dexamethasone Co-medication in cancer patients undergoing chemotherapy causes substantial immunomodulatory effects with implications for chemo-immunotherapy strategies, *Oncoimmunology* **5**, e1066062 (2016).
- [43] I. J. Elenkov, Glucocorticoids and the Th1/Th2 balance, *Ann. N. Y. Acad. Sci.* **1024**, 138 (2004).
- [44] C. Karagiannidis, M. Akdis, P. Holopainen, N. J. Woolley, G. Hense, B. Rückert, P.-Y. Mantel, G. Menz, C. A. Akdis, K. Blaser, and C. B. Schmidt-Weber, Glucocorticoids up-regulate foxp3 expression and regulatory T cells in asthma, *J. Allergy Clin. Immunol.* **114**, 1425 (2004).
- [45] G. Brand, Die Bedeutung der Spezifität von Immunreaktionen [The importance of the specificity of immune reactions], *Zentralbl. Bakteriol. Orig. A* **227**, 167 (1974).
- [46] M. Scurr, K. Ladell, M. Besneux, A. Christian, T. Hockey, K. Smart, H. Bridgeman, R. Hargest, S. Phillips, M. Davies, D. Price, A. Gallimore, and A. Godkin, Highly prevalent colorectal cancer-infiltrating LAP+ Foxp3- T cells exhibit more potent immunosuppressive activity than Foxp3+ regulatory T cells, *Mucosal Immunology* **7**, 428 (2014).
- [47] J. Kerzerho, H. Maazi, A. O. Speak, N. Szely, V. Lombardi, B. Khoo, S. Geryak, J. Lam, P. Soroosh, J. van Snick, and O. Akbari, Programmed cell death ligand 2 regulates TH9 differentiation and induction of chronic airway hyperreactivity, *J. Allergy Clin. Immunol.* **131**, 1048 (2013).
- [48] K. Hirahara, M. Yamashita, C. Iwamura, K. Shinoda, A. Hasegawa, H. Yoshizawa, H. Koseki, F. Gejyo, and T. Nakayama, Repressor of GATA regulates TH2-driven allergic airway inflammation and airway hyperresponsiveness, *J. Allergy Clin. Immunol.* **122**, 512 (2008).
- [49] W. W. Busse, W. J. Morgan, P. J. Gergen, H. E. Mitchell, J. E. Gern, A. H. Liu, R. S. Gruchalla, M. Kattan, S. J. Teach, J. A. Pongratic, J. F. Chmiel, S. F. Steinbach, A. Calatroni, A. Togias, K. M. Thompson, S. J. Szefer, and C. A. Sorkness, Randomized trial of omalizumab (Anti-IgE) for asthma in inner-city children, *N. Engl. J. Med.* **364**, 1005 (2011).
- [50] Y. Zhao, J. Yang, Y.-D. Gao, and W. Guo, Th17 immunity in patients with allergic asthma, *Int. Arch. Allergy Immunol.* **151**, 297 (2010).
- [51] J. R. Murdoch and C. M. Lloyd, Resolution of allergic airway inflammation and airway hyperreactivity is mediated by IL-17-producing  $\{\gamma\}\{\delta\}$ T cells, *Am. J. Respir. Crit. Care Med.* **182**, 464 (2010).
- [52] S. J. Szabo, B. M. Sullivan, S. L. Peng, and L. H. Glimcher, Molecular mechanisms regulating th1 immune responses, *Annu. Rev. Immunol.* **21**, 713 (2003).
- [53] V. Golubovskaya and L. Wu, Different subsets of T cells, memory, effector functions, and CAR-T immunotherapy, *Cancers* **8**, 36 (2016).
- [54] U. E. Schaible, H. L. Collins, and S. H. Kaufmann, Confrontation between intracellular bacteria and the immune system, *Adv. Immunol.* **71**, 267 (1999).
- [55] S. C. Cowley, E. Hamilton, J. A. Frelinger, J. Su, J. Forman, and K. L. Elkins, CD4-CD8- T cells control intracellular bacterial infections both in vitro and in vivo, *J. Exp. Med.* **202**, 309 (2005).
- [56] R. V. Luckheeram, R. Zhou, A. D. Verma, and B. Xia, CD4+ T Cells: Differentiation and functions, *Clin. Dev. Immunol.* **2012**, 925135 (2012).
- [57] A. S. Duddu, S. Sahoo, S. Hati, S. Jhunjunwala, and M. K. Jolly, Multi-stability in cellular differentiation enabled by a network of three mutually repressing master regulators, *J. R. Soc., Interface* **17**, 20200631 (2020).
- [58] R. Dantzer, Cytokine, sickness behavior, and depression, *Immunol. Allergy Clin. North Am.* **29**, 247 (2009).
- [59] M. Göttlicher, S. Heck, and P. Herrlich, Transcriptional cross-talk, the second mode of steroid hormone receptor action, *J. Mol. Med.* **76**, 480 (1998).
- [60] I. Bains, R. Antia, R. Callard, and A. J. Yates, Quantifying the development of the peripheral naive CD4+ T-Cell pool in humans, *Blood* **113**, 5480 (2009).
- [61] M. Feng and M. K. Gilson, Enhanced diffusion and chemotaxis of enzymes, *Annu. Rev. Biophys.* **49**, 87 (2020).
- [62] M. J. Miller, S. H. Wei, I. Parker, and M. D. Cahalan, Two-photon imaging of lymphocyte motility and antigen response in intact lymph node, *Science (New York, NY)* **296**, 1869 (2002).
- [63] S. Y. Qi, J. T. Groves, and A. K. Chakraborty, Synaptic pattern formation during cellular recognition, *Proc. Natl. Acad. Sci. USA* **98**, 6548 (2001).
- [64] J.-M. Anaya, Y. Shoenfeld, A. Rojas-Villarraga, R. A. Levy, and R. Cervera (Eds.), *Autoimmunity From Bench to Bedside* (El Rosario University Press, Bogota, Colombia, 2013).
- [65] J. Bezuidenhout and J. W. Schneider, in *Tuberculosis: A Comprehensive Clinical Reference*, edited by H. S. Schaaf, A. I. Zumla, J. M. Grange, M. C. Raviglione, W. W. Yew, J. R. Starke, M. Pai, and P. R. Donald (W.B. Saunders, Edinburgh, 2009), p. 117.
- [66] J. D. Murray, *Mathematical Biology. II: Spatial Models and Biomedical Applications*, Interdisciplinary Applied Mathematics Vol. 18 (Springer-Verlag, New York, 2001).
- [67] D. R. Bush and A. K. Chattopadhyay, Contact Time Periods in Immunological Synapse., *Phys. Rev. E* **90**, 042706 (2014).
- [68] A. K. Chattopadhyay and N. J. Burroughs, Close Contact Fluctuations: The Seeding of Signalling Domains in the Immunological Synapse, *Europhys. Lett.* **77**, 48003 (2007).

- [69] S. Raychaudhuri, A. K. Chakraborty, and M. Kardar, Effective Membrane Model of the Immunological Synapse, *Phys. Rev. Lett.* **91**, 208101 (2003).
- [70] M. L. Dustin, T-cell activation through immunological synapses and kinapses, *Immunol. Rev.* **221**, 77 (2008).
- [71] D. Fouchet and R. Regoes, A population dynamics analysis of the interaction between adaptive regulatory t cells and antigen presenting cells, *PLoS ONE* **3**, e2306 (2008).
- [72] S. M. C. Spoorenberg, V. H. M. Deneer, J. C. Grutters, A. E. Pulles, G. P. P. Voorn, G. T. Rijkers, W. J. W. Bos, and E. M. W. van de Garde, Pharmacokinetics of oral vs. intravenous dexamethasone in patients hospitalized with community-acquired pneumonia, *Br. J. Clin. Pharmacol.* **78**, 78 (2014).
- [73] D. E. Becker, Basic and clinical pharmacology of glucocorticosteroids, *Anesth. Prog.* **60**, 25 (2013).
- [74] T. R. Brophy, J. McCafferty, J. H. Tyrer, and M. J. Eadie, Bioavailability of oral dexamethasone during high dose steroid therapy in neurological patients, *Eur. J. Clin. Pharmacol.* **24**, 103 (1983).
- [75] D. Hsu and C. Katelaris, Long-term management of patients taking immunosuppressive drugs, *Aust. Prescriber* **32**, 68 (2009).
- [76] F. F. Fagnoni, L. Lozza, C. Zibera, A. Zambelli, L. Ponchio, N. Gibelli, B. Oliviero, L. Pavesi, R. Gennari, R. Vescovini, P. Sansoni, G. da Prada, and G. Robustelli Della Cuna, T-cell dynamics after high-dose chemotherapy in adults: elucidation of the elusive CD8+ subset reveals multiple homeostatic t-cell compartments with distinct implications for immune competence, *Immunology* **106**, 27 (2002).
- [77] See Supplemental Material at <http://link.aps.org/supplemental/10.1103/PhysRevE.103.062401> to follow time evolution with the dynamics of all the coarse grain network elements both in the presence and absence of glucocorticoid, the immune phase diagram of CD4+ T cell, and other data analysis.
- [78] S. M. Kaech, E. J. Wherry, and R. Ahmed, Effector and memory T-cell differentiation: Implications for vaccine development, *Nat. Rev. Immunol.* **2**, 251 (2002).
- [79] T. Lorenzi, R. H. Chisholm, M. Melensi, A. Lorz, and M. Delitala, Mathematical model reveals how regulating the three phases of T-cell response could counteract immune evasion, *Immunology* **146**, 271 (2015).
- [80] I. Gutcher and B. Becher, APC-derived cytokines and T cell polarization in autoimmune inflammation, *J. Clin. Invest.* **117**, 1119 (2007).
- [81] J. D. Milner, S. C. Kent, T. A. Ashley, S. B. Wilson, J. L. Strominger, and D. A. Hafler, Differential responses of invariant V $\alpha$ 24J $\alpha$ Q T cells and MHC class II-restricted CD4+ T cells to dexamethasone, *J. Immunol.* **163**, 2522LP (1999).
- [82] P. Sacerdote, Opioids and the immune system, *Palliat. Med.* **20**, s9 Suppl 1 (2006).
- [83] S. Tavakolpour, S. M. Alavian, and S. Sali, Hepatitis B Reactivation during immunosuppressive therapy or cancer chemotherapy, management, and prevention: A comprehensive review-screened, *Hepatitis Mon.* **16**, e35810 (2016).
- [84] S. A. Gonzalez and R. P. Perrillo, Hepatitis B virus reactivation in the setting of cancer chemotherapy and other immunosuppressive drug therapy, *Clin. Infect. Dis.* **62**, S306 (2016).
- [85] R. M. Paragliola, G. Papi, A. Pontecorvi, and S. M. Corsello, Treatment with synthetic glucocorticoids and the hypothalamus-pituitary-adrenal axis, *Int. J. Mol. Sci.* **18**, 2201 (2017).
- [86] I. Bose and M. Pal, Criticality in cell differentiation, *J. Biosci.* **42**, 683 (2017).
- [87] M. Mojtahedi, A. Skupin, J. Zhou, I. G. Castaño, R. Y. Y. Leong-Quong, H. Chang, K. Trachana, A. Giuliani, and S. Huang, Cell fate decision as high-dimensional critical state transition, *PLoS Biol.* **14**, e2000640 (2016).
- [88] M. Scheffer, J. Bascompte, W. A. Brock, V. Brovkin, S. R. Carpenter, V. Dakos, H. Held, E. H. van Nes, M. Rietkerk, and G. Sugihara, Early-warning signals for critical transitions, *Nature (London)* **461**, 53 (2009).
- [89] F. Buttgerit, M. Wehling, and G. R. Burmester, A new hypothesis of modular glucocorticoid actions: steroid treatment of rheumatic diseases revisited, *Arthritis Rheum.* **41**, 761 (1998).
- [90] D. Huscher, K. Thiele, E. Gromnica-Ihle, G. Hein, W. Demary, R. Dreher, A. Zink, and F. Buttgerit, Dose-related patterns of glucocorticoid-induced side effects, *Ann. Rheum. Dis.* **68**, 1119 (2009).
- [91] N. Gegechkori, L. Haines, and J. J. Lin, Long-term and latent side effects of specific cancer types, *Med. Clin. North Am.* **101**, 1053 (2017).
- [92] S. Kusumoto, Y. Tanaka, M. Mizokami, and R. Ueda, Reactivation of hepatitis b virus following systemic chemotherapy for malignant lymphoma, *Int. J. Hematol.* **90**, 13 (2009).
- [93] D. Shoup, G. Lipari, and A. Szabo, Diffusion-controlled bimolecular reaction rates. the effect of rotational diffusion and orientation constraints, *Biophys. J.* **36**, 697 (1981).
- [94] L. Gustavson and L. Benet, in *Adrenal Cortex: Butterworths International Medical Reviews: Clinical Endocrinology*, edited by D. C. Anderson and J. S. D. Winter (Elsevier Science, 1985), p. 235.
- [95] N. Bairagi, S. Chatterjee, and J. Chattopadhyay, Variability in the secretion of corticotropin-releasing hormone, adrenocorticotrophic hormone and cortisol and understandability of the hypothalamic-pituitary-adrenal axis dynamics—a mathematical study based on clinical evidence, *Math. Med. Biol.* **25**, 37 (2008).